Building change detection in satellite stereo imagery based on belief functions

Jiaojiao Tian, Peter Reinartz
Remote Sensing Technology Institute
German Aerospace Center
Oberpfaffenhofen, Germany 82234
Email: jiaojiao.tian, peter.reinartz@dlr.de

Jean Dezert
ONERA - The French Aerospace Lab
Chemin de la Hunière
Palaiseau, France F-91761
Email: jean.dezert@onera.fr

***Abstract*—3D Building change detection has become a popular research topic along with the improvement of image quality and computer science. When only building changes are of interest, both the multi-temporal images and Digital Surface Models provide valuable but not comprehensive information in the change detection procedure. Therefore, in this paper, belief functions have been adopted for fusing information from these two sources. In the first step, two change indicators are proposed by focusing on building changes. Both indicators have been projected to a sigmoid curve, in which both the concordance and discordance indexes are considered. In order to fuse the concordance and discordance indexes and further fuse the two change indicators, two belief functions are considered. One is the original Dempster-Shafer Theory (DST), and the most recent one is Dezert-Smarandache Theory (DSmT). This paper shows how these belief-based frameworks can help in building change detection problem. Besides using different belief functions in obtaining the global BBAs, four decision-making criteria are tested to extract final building change masks. The results have been validated by compared to the manually extracted change reference mask.**

I. Introduction

Accurate and efficient detection of changes is of great importance for urban monitoring, which is also an important research field in remote sensing. Change detection methods on large scale land cover monitoring have been intensively studied and reviewed [1][2]. Along with the ascending of image spectral and temporal resolution, the expectation on automatic change detection has progressively increased, not only on results accuracy, but also on the efficiency and robustness of the methods. Moreover, change detection for a specific target of interest, like buildings is becoming an important research topic. In small scale 2D change detection, which is performed based on only 2D multi-temporal spectral images, problems arise due to misdetections caused by irrelevant changes. The influence of these irrelevant changes is growing as higher resolution images showing more details. Therefore, in this paper, we will further work on satellite multispectral and stereo images, which provides both spectral and height change information.

Adopting satellite stereo imagery for 3D change detection is an exciting and challenging task. Benefiting from improved data quality and advanced computer vision technique, the quality of the generated Digital Surface Models (DSMs) has been largely improved and it is possible to detect changes even for small objects, like single buildings. On the other side, the DSMs may still exhibit some outliers resulting in occlusions within the stereo/multi views. Several approaches have been proposed for DSM assisted change detection [3], [4], [5], [6]. According to our previous research results, the belief functions introduced in DST allow to work more efficiently and robustly in urban building change detection with very high resolution satellite images [7]. So far, only a basic DS fusion model has been proposed in [6] to define the Basic Belief Assignments (BBAs) thanks to a sigmoid curve considering only the concordance index. Improvement of this DS fusion model for BBAs construction is proposed in this paper to achieve better performance by considering both the concordance and discordance indexes. Since DSmT [8] has been developed in last years as an interesting alternative to DST to circumvent problems of Dempster-Shafer's (DS) rule of combination [9], we also investigate the possibility of using the Proportiobnal Conflict Redistribution Rule #6 (PCR6) of DSmT in our application.

II. Basics of belief functions

Detailed presentations of DST and DSmT can be found in [8], [9] and [10]. Let Θ be a frame of discernment of a problem under consideration. $\Theta = \{\theta_1, \theta_2, \ldots, \theta_N\}$ consists of a list of N exhaustive and mutually exclusive elements θ_i, $i = 1, 2, \ldots, N$. Each θ_i represents a possible state related to the problem we want to solve. The assumption of exhaustivity and mutual exclusivity of elements of Θ is classically referred as *Shafer's model* of the frame Θ. A BBA also called a belief mass function (or just a mass for short), is a mapping $m(.) : 2^\Theta \rightarrow [0, 1]$ from the power set[1] of Θ denoted 2^Θ to $[0, 1]$, that verifies [10]:

$$m(\emptyset) = 0 \quad \text{and} \quad \sum_{X \in 2^\bullet} m(X) = 1 \tag{1}$$

$m(X)$ represents the mass of belief exactly committed to X. An element $X \in 2^\Theta$ is called a focal element if and only if $m(X) > 0$. In DST, the combination (fusion) of several independent sources of evidences is done with Dempster-Shafer[2] (DS) rule of combination, assuming that the sources are not in total conflict[3]. DS combination of two independent BBAs

[1]The power set is the set of all subsets of Θ, empty set included.

[2]Although the rule has been proposed originally by Dempster, we call it Dempster-Shafer rule because it has been widely promoted by Shafer in DST.

[3]otherwise DS rule is mathematically not defined because of 0/0 indeterminacy.

978-1-4799-6652-3/15/$31.00~ ©2015 IEEE

$m_1(.)$ and $m_2(.)$, denoted symbolically by $DS(m_1, m_2)$, is defined by $m^{DS}(\emptyset) = 0$, and for all $X \in 2^\Theta \setminus \{\emptyset\}$ by:

$$m^{DS}(X) = \frac{1}{1 - K^{DS}} \sum_{\substack{X_1, X_2 \in 2^\Theta \\ X_1 \cap X_2 = X}} m_1(X_1) m_2(X_2) \quad (2)$$

where the total degree of conflict K^{DS} is given by

$$K^{DS} \triangleq \sum_{\substack{X_1, X_2 \in 2^\bullet \\ X_1 \cap X_2 = \emptyset}} m_1(X_1) m_2(X_2) \quad (3)$$

A discussion on the validity of DS rule and its incompatibility with Bayes fusion rule for combining Bayesian BBAs can be found in [9], [11], [12]. To circumvent the problems of DS rule, Smarandache and Dezert (see [8], Vol. 2, Chap. 1), then Martin and Osswald (see [8], Vol. 2, Chap. 2) have developed in DSmT [8] two fusion rules called PCR5 and PCR6 based on the proportional conflict redistribution (PCR) principle which consists

1) to apply the conjunctive rule;
2) calculate the total or partial conflicting masses;
3) then redistribute the (total or partial) conflicting mass proportionally on non-empty sets according to the integrity constraints one has for the frame Θ.

This PCR principle transfers the conflicting mass only to the elements involved in the conflict and proportionally to their individual masses, so that the specificity of the information is not degraded. Because the proportional transfer can be done in two different ways, this has yielded to two different fusion rules. It has been proved in [13] that only PCR6 rule is compatible with frequentist probability estimation, and that is why we recommend its use in the applications. PCR5 and PCR6 rules simplify greatly and coincide for the combination of two sources. In this case, the PCR6 combination is obtained by taking $m^{PCR6}(\emptyset) = 0$, and for all $X \neq \emptyset$ in 2^Θ by

$$m^{PCR6}(X) = \sum_{\substack{X_1, X_2 \in 2^\bullet \\ X_1 \cap X_2 = X}} m_1(X_1) m_2(X_2) + \sum_{\substack{Y \in 2^\bullet \setminus \{X\} \\ X \cap Y = \emptyset}} \left[\frac{m_1(X)^2 m_2(Y)}{m_1(X) + m_2(Y)} + \frac{m_2(X)^2 m_1(Y)}{m_2(X) + m_1(Y)} \right] \quad (4)$$

where all denominators in Eq. (4) are different from zero. If a denominator is zero, that fraction is discarded.

III. Building change detection models

A. Choice of the frame of discernment

We now use two sources (indicators) of evidences to solve our problem. As a preparation step, the indicators and focal elements have to be introduced. Two data sources are used for building change detection. One is the satellite images, which contain 2D spectral information. Here we use the Iteratively Reweighted Multivariate Alteration Detection (IRMAD) [14] to highlight changes from the spectral images. The other is the robust height difference which can be calculated from the two Digital Surface Models (DSMs) [6]. Detail of the DSM generation procedure and the characters of the DSMs quality have been described in [5]. As it has been explained in [6], we suppose that new, demolished or changed buildings exhibit both height changes and spectral changes. The seasonal changes will only influence the spectral images. Therefore, for building change detection, we consider the following three classes (hypotheses) to define our frame of discernment satisfying Shafer's model: $\Theta = \{\theta_1 \triangleq$ Pixel $\in$ BuildingChange,$\theta_2 \triangleq$ Pixel $\in$ OtherChange,$\theta_3 \triangleq$ Pixel $\in$ NoChange$\}$.

B. Sigmoidal model for BBA construction

BBAs construction is a prerequisite for the combination of sources of evidence. In our previous works [6], the BBAs were built based on sigmoid curves related with the concordance index only. In this paper, we improve our model to construct the BBAs thanks to sigmoidal models for both concordance and discordance indexes following idea proposed in [15]. As explained in [6], the original sigmoid curve is defined as

$$f_{(\tau,T)}(x) = 0.99/(1 + e^{-\frac{x-T}{\tau}}) \quad (5)$$

where x is the original value of each indicator. Two parameters T and τ are used to control the symmetry point and the slope of the sigmoid function. The symmetry point indicates a certainty of 50%. The construction of BBAs is explained in [15] and adopted in this paper. In [15] these two parameters T and τ are manually given to sigmoid curve. Here, the multi-level Otsu's thresholding method [16] is used to get symmetry points for both concordance index and discordance index. Otsu's algorithm defines that an image is composed of objects and background. A discriminant analysis is performed by minimizing the intra-class variance. When three classes are of interest, two threshold values are expected. Otsu's method can be extended to

$$\sigma^2_\omega(T_1, T_2) = \omega_1 \sigma^2_1(T_1, T_2) + \omega_2 \sigma^2_2(T_1, T_2) + \omega_3 \sigma^2_3(T_1, T_2) \quad (6)$$

The weights ω_i are the probabilities obtained from the image histogram that are separated by the thresholds T_1 and T_2. σ_i are the variances of the three classes. T_1 and T_2 can be used as the symmetry points of discordance and concordance index respectively. Thus, using height change index as example, the BBAs for discordance and concordance height change index are presented as $a_{\Delta H}$ and $b_{\Delta H}$

$$a_{\Delta H} = f_{\tau, T_1}(\Delta H), \quad \text{and} \quad b_{\Delta H} = f_{-\tau, T_2}(\Delta H) \quad (7)$$

The factor τ is calculated with a sample value ($\Delta H = 1$, $a_{\Delta H} = 0.1$), which means 1 meter height change indicates 10% probability to be building changes. The BBAs for discordance and concordance image change index are built similarly. Differences appearing in 2D images give a concordance indication for all changes, which include the building changes and other changes $(\theta_1 \cup \theta_2)$. In this paper the changes from images are named ΔImg.

C. BBAs construction using concordance and discordance

The BBAs related with the concordance and discordance indexes are combined to get the global BBA related to each source of evidence. These global BBAs will then be used as input for solving the change detection problem thanks to their combination. In the Tables I and II, we present the two ways of construction of the BBAs of the sources of evidence based

TABLE I. BBA CONSTRUCTION FOR HEIGHT CHANGE INDICATOR ΔH. $[K_{\Delta H} = a_{\Delta H} b_{\Delta H}]$

Focal Elem.	$m_1(.)$	$m'_1(.)$	$m_1^{DS}(.)$	$m_1^{PCR6}(.)$
θ_1	$a_{\Delta H}$	0	$\frac{a_{\Delta H}(1-b_{\Delta H})}{1-K_{\Delta H}}$	$a_{\Delta H}(1-b_{\Delta H}) + \frac{a_{\Delta H} K_{\Delta H}}{a_{\Delta H}+b_{\Delta H}}$
θ_2	0	0	0	0
θ_3	0	0	0	0
$\theta_1 \cup \theta_2$	0	0	0	0
$\theta_2 \cup \theta_3$	0	$b_{\Delta H}$	$\frac{(1-a_{\Delta H}) b_{\Delta H}}{1-K_{\Delta H}}$	$(1-a_{\Delta H}) b_{\Delta H} + \frac{b_{\Delta H} K_{\Delta H}}{a_{\Delta H}+b_{\Delta H}}$
$\theta_1 \cup \theta_2 \cup \theta_3$	$1-a_{\Delta H}$	$1-b_{\Delta H}$	$\frac{(1-a_{\Delta H})(1-b_{\Delta H})}{1-K_{\Delta H}}$	$(1-a_{\Delta H})(1-b_{\Delta H})$

TABLE II. BBA CONSTRUCTION FOR IMAGE CHANGE INDICATOR ΔImg. $[K_{\Delta Img} = a_{\Delta Img} b_{\Delta Img}]$

Focal Elem.	$m_2(.)$	$m'_2(.)$	$m_2^{DS}(.)$	$m_2^{PCR6}(.)$
θ_1	0	0	0	0
θ_2	0	0	0	0
θ_3	0	$b_{\Delta Img}$	$\frac{(1-a_{\Delta Img}) b_{\Delta Img}}{1-K_{\Delta Img}}$	$(1-a_{\Delta Img}) b_{\Delta Img} + \frac{b_{\Delta Img} K_{\Delta Img}}{a_{\Delta Img}+b_{\Delta Img}}$
$\theta_1 \cup \theta_2$	$a_{\Delta Img}$	0	$\frac{a_{\Delta Img}(1-b_{\Delta Img})}{1-K_{\Delta Img}}$	$a_{\Delta Img}(1-b_{\Delta Img}) + \frac{a_{\Delta Img} K_{\Delta Img}}{a_{\Delta Img}+b_{\Delta Img}}$
$\theta_2 \cup \theta_3$	0	0	0	0
$\theta_1 \cup \theta_2 \cup \theta_3$	$1-a_{\Delta Img}$	$1-b_{\Delta Img}$	$\frac{(1-a_{\Delta Img})(1-b_{\Delta Img})}{1-K_{\Delta Img}}$	$(1-a_{\Delta Img})(1-b_{\Delta Img})$

either on DS or on PCR6 rules of combination for the height change indicator (i.e. the first source of evidence) and the image change indicator (i.e. the second source of evidence). In Table I, $m_1(.)$ and $m'_1(.)$ represent the concordance and discordance BBAs from ΔH, whereas in Table II $m_2(.)$ and $m'_2(.)$ represent the concordance and discordance BBAs from images.

Here for comparison of the two belief functions, these two BBAs are fused with both DS and PCR6 fusion rules. The fusion rules for height change indicator and image change indicator are explained in Table I and Table II. In Table I, the m_1 and m'_1 represent the concordance and discordance BBAs from ΔH. In Table II we use m_2 and m'_2 to represent the concordance and discordance BBAs from images.

D. BBAs combination for building change detection

From the previous step of BBAs modelings, each pixel will get two sets of BBAs to combine resulting from Table I and II. More precisely, we will have to combine either $\{m_1^{DS}(.), m_2^{DS}(.)\}$ if DS rule is preferred for the BBA modeling, or $\{m_1^{PCR6}(.), m_2^{PCR6}(.)\}$ if PCR6 rule is adopted. These BBAs have been represented by a_1, b_1, c_1 and a_2, b_2, c_2 in Table III. Based on different BBAs and fusion methods, four sets of global BBAs can be computed from Table III.

$$\begin{aligned} G_1 &= DS\{m_1^{DS}(.), m_2^{DS}(.)\} \\ G_2 &= PCR6\{m_1^{DS}(.), m_2^{DS}(.)\} \\ G_3 &= DS\{m_1^{PCR6}(.), m_2^{PCR6}(.)\} \\ G_4 &= PCR6\{m_1^{PCR6}(.), m_2^{PCR6}(.)\} \end{aligned} \tag{8}$$

After the fusion step, each pixel in the images will get a certain degree of belief for all focal elements. Based on the these BBAs, a final decision can be made. DST and DSmT have different approaches to get this final decision. In this paper four decision criteria are tested. More precisely, we have evaluated the maximum of global BBAs (Max_Bel), maximum of plausibility (Max_Pl), maximum of betting probabilities (Max_BetP) and the maximum of DSmP (Max_DSmP),), see [8] (Vol. 3, Chap. 3) and [10] for the mathematical definitions of $Bel(.)$, $Pl(.)$, $BetP(.)$ and $DSmP(.)$ functions.

TABLE III. FUSION MODELS FOR BUILDING CHANGE DETECTION.

Focal Elem.	$m_1(.)$	$m_2(.)$	$m_{12}^{DS}(.)$	$m_{12}^{PCR6}(.)$
θ_1	a_1	0	$\frac{a_1(b_1+b_3)}{1-a_1 b_2}$	$a_1(b_1+b_3) + \frac{a_1 a_1 b_2}{a_1+b_2}$
θ_2	0	0	$\frac{a_2 b_1}{1-a_1 b_2}$	$a_2 b_1$
θ_3	0	b_2	$\frac{(a_2+a_3) b_2}{1-a_1 b_2}$	$(a_2+a_3) b_2 + \frac{b_2 a_1 b_2}{a_1+b_2}$
$\theta_1 \cup \theta_2$	0	b_1	$\frac{a_3 b_1}{1-a_1 b_2}$	$a_3 b_1$
$\theta_2 \cup \theta_3$	a_2	0	$\frac{a_2 b_3}{1-a_1 b_2}$	$a_2 b_3$
Θ	a_3	b_3	$\frac{a_3 b_3}{1-a_1 b_2}$	$a_3 b_3$

IV. EXPERIMENTS

The two proposed BBAs modelings and fusion methods (based on DS and PCR6 rules) have been tested on one real dataset. The dataset and the results from each step are detailed in this section.

A. Datasets

The experimental dataset for this research work are displayed in Fig.1. It consists of two pairs of IKONOS stereo imagery captured at February 2006 and May 2011 respectively. As a pre-processing step, all data have been correctly radiometrically and geographically co-registered as described in [6]. As shown in Fig. 1, this is a normal building change example. Several buildings have been built on flat surface. The generated DSMs are displayed in Fig. 1c and d.

B. Results and evaluation

As the first step, BBAs from image change and height change are extracted and refined based on DS fusion and PCR6 fusion rules. The four sets of global BBAs are prepared corresponding to Eq. (8). Among them the BBA for the focal element θ_1 (Building change) are shown in Fig. 2. The accuracy of these BBAs have been evaluated by area under Receiver Operating Characteristic curve (AUC). The AUC has been recorded on this figure as the caption of each subfigure. An advantage of PCR6 can be proved here. It has to be noted that the AUCs obtained here are much higher than using only height (AUC = 0.9299) [6] or spectral information (AUC=0.8823), and generally better than the fusion result described in [6] (AUC=0.9621).

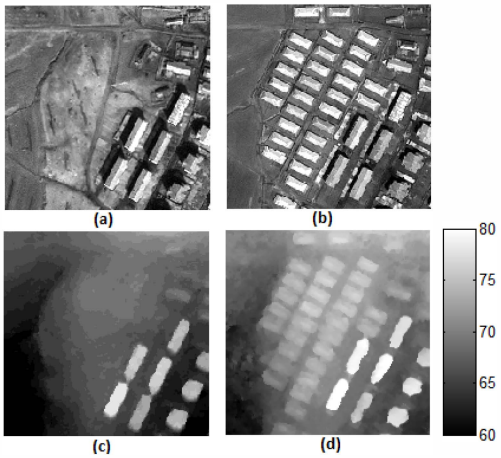

Fig. 1. Experimental dataset: a) panchromatic image from date1; b) panchromatic image from date2; c) DSM from date1; (d) DSM from date2.

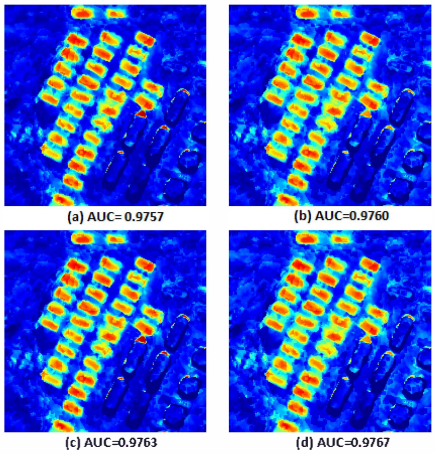

Fig. 2. Four global BBAs sets (a) G_1; (b)G_2; (c)G_3; (d)G_4.

Besides the AUC comparison, the building change masks extracted from these four global BBAs sets are compared and evaluated. Each global BBA set can generate four building change mask based on these four decision make criteria. These building change masks are evaluated based on Kappa statistic (KA) and true detected rate (TR). In this paper $\text{TR} = \frac{\text{detected positive}}{\text{true positive}} * 100\%$. The comparison results of TR and KA values are shown in Table IV. From Table IV, one sees that, G_3 and G_4 are more advantageous than G_1 and G_2. However, the highest KA is obtained by G_1 by taking the Max_Pl. However, in this paper, only the reference data for building changes are available. For better understanding these four global BBAs and decision making criteria, reference data of all three focal elements θ_1, θ_2 and θ_3 are required.

TABLE IV. CHANGE MASKS EVALUATION FROM FOUR GLOBAL BBAS.

	G_1		G_2		G_3		G_4	
	TR [%]	KA	TR[%]	KA	TR [%]	KA	TR [%]	KA
Max_Bel	93.35	0.7729	93.35	0.7729	93.39	0.7725	93.39	0.7724
Max_Pl	93.23	0.7768	93.23	0.7762	93.23	0.7763	93.25	0.7756
Max_BetP	93.28	0.7747	93.32	0.7762	93.32	0.7745	93.32	0.7741
Max_DSmP	93.30	0.7739	93.30	0.7734	93.30	0.7737	93.34	0.7734

V. CONCLUSIONS

Belief functions are good choices for DSM assisted change detection. Firstly, once the BBA construction is well done, it can be robustly used for other images in other regions efficiently. Secondly, this fusion approach matches well with the characteristics of our research topic. Since height information is important for separating high/low level objects. Satellite images directly highlight all changes on the land surface. None of these two sources of information can easily and directly lead to a reliable decision on building changes, which matches with the initial idea of belief functions. Generally speaking, both DST and DSmT frameworks offer the possibility to reach a high accuracy result, and PCR6 looks advantageous when a larger conflict exists between the different sources of evidence. More experiments are under progress to provide a finer quantitative comparative analysis in a forthcoming publication.

REFERENCES

[1] A. Singh, "Digital change detection techniques using remotely-sensed data," *Int. J. Remote Sens.*, vol. 10, no. 6, pp. 989–1003, 1989.

[2] D. Lu, P. Mausel, E. Brondizio, and E. Moran, "Change detection techniques," *Int. J. Remote Sens.*, vol. 25, no. 12, pp. 2365–2407, 2004.

[3] F. Rottensteiner, J. Trinder, S. Clode, and K. Kubik, "Using the Dempster–Shafer method for the fusion of LIDAR data and multi-spectral images for building detection," *Information Fusion*, vol. 6, no. 4, pp. 283–300, 2005.

[4] N. Champion, F. Rottensteiner, L. Matikainen, X. Liang, J. Hyyppä, and B. Olsen, "A test of automatic building change detection approaches," *Proc. of CMRT09*, pp. 03–04, 2009.

[5] J. Tian, P. Reinartz, P. d'Angelo, and M. Ehlers, "Region-based automatic building and forest change detection on Cartosat-1 stereo imagery," *ISPRS J. Photogramm. and Remote Sens.*, vol. 79, pp. 226–239, 2013.

[6] J. Tian, S. Cui, and P. Reinartz, "Building change detection based on satellite stereo imagery and digital surface models," *IEEE Trans. Geosci. Remote Sens.*, vol. 52, no. 1, pp. 406–417, 2014.

[7] J. Tian and P. Reinartz, "Comparison of two fusion based building change detection methods using satellite stereo imagery and dsms," *ISPRS-Int. Archives the Photogramm., Remote Sens. and Spatial Information Sciences*, vol. XL-7, no. W1, pp. 103–108, 2013.

[8] F. Smarandache and J. Dezert, *Advances and Applications of DSmT for Information Fusion*. American Research Press, Rehoboth, NM, U.S.A, 2004–2009, vol. 1–3.

[9] J. Dezert and A. Tchamova, "On the validity of Dempster's fusion rule and its interpretation as a generalization of Bayesian fusion rule," *Int. J. Intell. Syst.*, vol. 29, no. 3, pp. 223–252, 2014.

[10] G. Shafer, *A mathematical theory of evidence*. Princeton university press Princeton, 1976.

[11] J. Dezert, P. Wang, and A. Tchamova, "On the validity of Dempster-Shafer theory," in *Proc. of FUSION 2012*, 2012, pp. 655–660. [Online]. Available: http://fs.gallup.unm.edu//DSmT.htm

[12] A. Tchamova and J. Dezert, "On the behavior of Dempster's rule of combination and the foundations of Dempster-Shafer theory," in *Proc. of IS 2012*, 2012, pp. 108–113.

[13] F. Smarandache and J. Dezert, "On the consistency of PCR6 with the averaging rule and its application to probability estimation," in *Proc. of FUSION 2013*, 2013, pp. 1119–1126.

[14] A. A. Nielsen, "The regularized iteratively reweighted MAD method for change detection in multi-and hyperspectral data," *IEEE Trans. Image Process.*, vol. 16, no. 2, pp. 463–478, 2007.

[15] J. Dezert and J.-M. Tacnet, "Sigmoidal model for belief function-based electre tri method," in *Belief Functions: Theory and Applications*, 2012, pp. 401–408.

[16] N. Otsu, "A threshold selection method from gray-level histograms," *IEEE Trans. Syst., Man, Cybern.*, vol. 9, no. 1, pp. 62–66, 1975.